# Tilting mode relaxation in the electron paramagnetic resonance of oxygen-isotope-substituted $La_{2-x}Sr_xCuO_4:Mn^{2+}$

A. Shengelaya, H. Keller, and K. A. Müller
*Physik-Institut der Universität Zürich, CH-8057 Zürich, Switzerland*

B. I. Kochelaev
*Department of Physics, Kazan State University, Kazan, 420008, Russia*

K. Conder
*Laboratorium für Festkörperphysik, ETH Zürich, CH-8093 Zürich, Switzerland*
(Received 24 February 2000; published 20 March 2001)

The electron paramagnetic resonance (EPR) of $Mn^{2+}$ doped into $La_{2-x}Sr_xCuO_4$ was used to probe the copper spin relaxation via the bottleneck effect for oxygen isotope ($^{16}O$ and $^{18}O$) substituted samples. The concentration range $x$ extended from 0.06 to 0.20 and the temperature dependence of the EPR linewidth was studied from 4 to 300 K. It was found that the EPR linewidth is larger for the $^{18}O$ isotope samples than for the $^{16}O$ samples. The isotope effect is pronounced at low temperatures and decreases with increasing Sr concentration. This effect is quantitatively explained by the $Cu^{2+}$ $S=1/2$ spin relaxation to the lattice via Dzyaloshinski terms coupled linearly to the local $Q_4/Q_5$ tilting modes of the $CuO_6$ octahedra as proposed by B. I. Kochelaev [J. Supercond. **12**, 53 (1999)]. The $Q_4/Q_5$ modes are coupled sterically to the $Q_2$ Jahn-Teller modes considered to be relevant for the (bi)polaron formation and thus for the high-temperature superconductivity.

DOI: 10.1103/PhysRevB.63.144513 PACS number(s): 74.72.Dn, 76.30.−v

## I. INTRODUCTION

The investigation of high-$T_c$ superconductors has, from a magnetic resonance point of view, until recently been dominated by nuclear magnetic resonance (NMR). The observation of electron paramagnetic resonance (EPR) is of great interest, because the time domain of observation of EPR is two to three orders of magnitude shorter than that of NMR. However, the application of EPR to high-$T_c$ cuprates was restricted owing to the absence of intrinsic EPR signals in these compounds. The reason of the EPR silence in the cuprates is due to the extremely large linewidth, which is estimated in the present study. The situation has improved recently, when the EPR from trapped three-spin polarons was observed in $La_{2-x}Sr_xCuO_4$, in which the presence of $Q_2$-type Jahn-Teller (JT) polarons were identified by Kochelaev *et al.*[2] in agreement with extended x-ray-absorption fine-structure (EXAFS) studies.[3] Another approach in the application of EPR to high-$T_c$ superconductors is to dope these compounds with small amounts of some paramagnetic ions which are used to probe the intrinsic behavior. One of the best candidates is Mn, which in the 2+ valent state gives a well defined signal and substitutes for the $Cu^{2+}$ in the $CuO_2$ plane. Recently, Kochelaev *et al.*[4] have intensively studied the EPR of $Mn^{2+}$ doped $La_{2-x}Sr_xCuO_4$. They found that the Mn ions are strongly coupled to the collective motion of the Cu spins (the so called bottleneck regime). The bottleneck regime allows to obtain substantial information on the dynamics of the copper electron spins in the $CuO_2$ plane.[4]

We decided to take advantage of the $Mn^{2+}$-doped $La_{2-x}Sr_xCuO_4$ and search for possible oxygen isotope effects on the EPR signal. We observed a large isotope effect on the EPR linewidth in the underdoped samples. The isotope effect decreases with Sr doping and practically disappears in the overdoped region. The observed large isotope effect can be quantitatively described by a symmetry invariant Hamiltonian in which the octahedral $Q_4$ and $Q_5$ tilting and tunneling modes are coupled linearly to Dzialoshinsky-type spin terms. The coupling constants can be estimated. This then allows an estimation of the intrinsic EPR relaxation time in the $La_{2-x}Sr_xCuO_4$ for the doped $CuO_2$ plane. Furthermore, the intrinsic $Q_4/Q_5$ tilting of the octahedra resulting from the $Q_2$ JT distortions deduced from EPR (Ref. 2) and EXAFS (Ref. 3) is underlined.

## II. EXPERIMENTAL DETAILS

The polycrystalline samples of $La_{2-x}Sr_xCu_{1-y}Mn_yO_4$ with $0.06 \leqslant x \leqslant 0.20$ and $0.01 \leqslant y \leqslant 0.04$ were prepared by the standard solid-state reaction method. Oxygen isotope substitution has been made at 800°C for 30 h in an oxygen pressure of ~1.0 bars. Oxygen isotope enrichment of the samples were determined using thermogravimetry. The $^{18}O$ samples have about 85% $^{18}O$ and 15% $^{16}O$. The EPR measurements were performed at 9.4 GHz using a Bruker ER-200D spectrometer equipped with an Oxford Instruments helium flow cryostat. The temperature was controlled between 4.2 and 300 K by an ITC-502 temperature controller. In order to avoid a signal distortion because of skin effects, the samples were ground and the powder was suspended in paraffin. It is important to note that the EPR spectra for the samples with different oxygen isotopes were taken with exactly the same spectrometer conditions. Special care was taken also to perform the experiments on samples with the same mass, mounted in identical sample tubes, etc. The re-

 

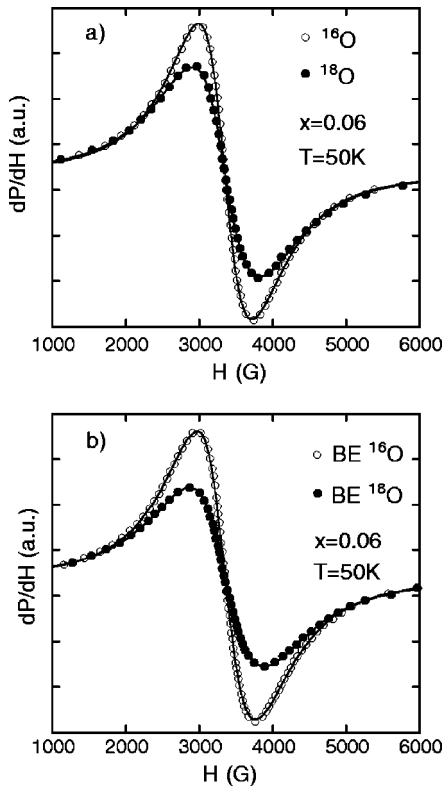


FIG. 1. (a) EPR signal of $^{16}$O and $^{18}$O samples of $La_{1.94}Sr_{0.06}Cu_{0.98}Mn_{0.02}O_4$ measured at $T=50$ K under identical experimental conditions. The fits to a Lorentzian line shape are represented by solid lines. (b) EPR signal of $^{16}$O and $^{18}$O samples of $La_{1.94}Sr_{0.06}Cu_{0.98}Mn_{0.02}O_4$ after isotope back exchange from $^{18}$O to $^{16}$O (BE $^{16}$O) and from $^{16}$O to $^{18}$O (BE $^{18}$O). One can see that the isotope effect is reversible.

producibility of the measured EPR signals was checked several times. Thus the EPR signals obtained for samples with different oxygen isotopes can be directly compared.

### III. EXPERIMENTAL RESULTS

We observed an EPR signal in all examined samples. The line shape of the signal is Lorentzian and symmetric throughout the whole temperature range. The resonance field corresponds to $g\sim 2$, a value very close to the $g$ factor for the $Mn^{2+}$ ion. Figure 1(a) shows typical EPR spectra for $x=0.06$, $y=0.02$ sample with different oxygen isotopes $^{16}$O and $^{18}$O. Investigation for Sr doping below 0.06 will be a subject to another publication.[5] From Fig. 1(a) one can see a difference between the EPR signals of the two isotope samples. Analysis of the spectra showed that the integral intensities of the EPR signals in two isotope samples are the same, but the linewidths are different. The linewidth for the $^{18}$O sample is larger than for the $^{16}$O sample, giving rise to different amplitudes for the EPR signal for two isotope samples. We performed measurements on back-exchanged samples in order to check whether the observed isotope effect is intrinsic. The corresponding results are presented in Fig. 1(b). It is seen that the isotope effect is completely reversible. We studied also the samples with different Mn concentration ($y=0.01,\ 0.04$) in order to clarify the role of Mn doping in the observed isotope effect. We found that the absolute value of linewidth changes with Mn concentration, however the isotope effect itself is independent on Mn content. This shows that $Mn^{2+}$ serves as an EPR probe and the observed isotope effect is intrinsic to $La_{2-x}Sr_xCuO_4$. Taking this into account we studied samples with a fixed Mn concentration of $y=0.02$ and different Sr doping.

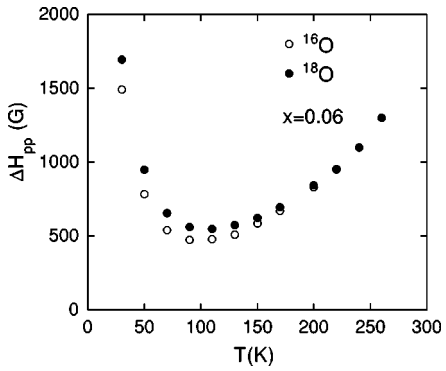


FIG. 2. Temperature dependence of the peak-to-peak EPR linewidth $\Delta H_{pp}$ for $^{16}$O and $^{18}$O samples of $La_{1.94}Sr_{0.06}Cu_{0.98}Mn_{0.02}O_4$.

Figure 2 shows the temperature dependence of the linewidth for the $x=0.06$ sample with different oxygen isotopes. With decreasing temperature the linewidth decreases, passes through a minimum at a temperature $T_{min}$ and increases again on further cooling. A similar temperature dependence was observed by Kochelaev *et al.*[4] in an EPR study of Mn-doped $La_{2-x}Sr_xCuO_4$ with $^{16}$O isotope. From Fig. 2 one can see that the observed isotope effect on the EPR linewidth is temperature dependent. The isotope effect is large at low temperatures and gradually disappears above $T_{min}$ at high temperatures.

We found that the isotope effect decreases with increasing Sr concentration. EPR spectra and the temperature dependence of the EPR linewidth for the more doped sample $x=0.10$ with different oxygen isotopes are shown in Figs. 3 and 4, respectively. One can see that the isotope effect is smaller than for the $x=0.06$ sample, but the qualitative behavior is the same. We also measured optimally doped and

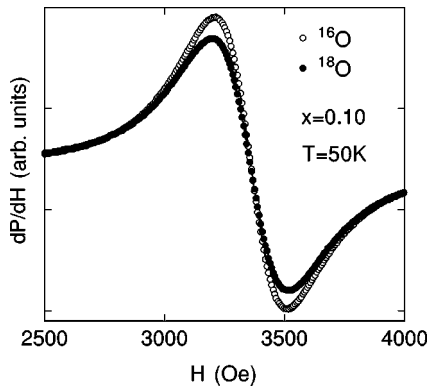


FIG. 3. EPR signal of $^{16}$O and $^{18}$O samples of $La_{1.90}Sr_{0.10}Cu_{0.98}Mn_{0.02}O_4$ measured at $T=50$ K under identical experimental conditions.

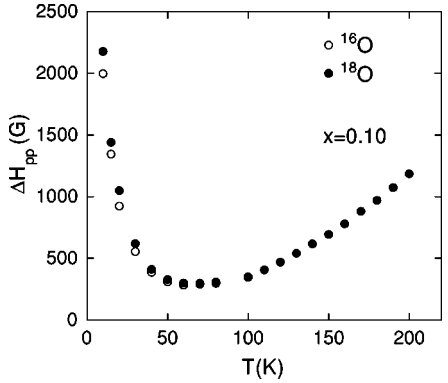


FIG. 4. Temperature dependence of the peak-to-peak EPR linewidth $\Delta H_{pp}$ for $^{16}O$ and $^{18}O$ samples of $La_{1.90}Sr_{0.10}Cu_{0.98}Mn_{0.02}O_4$.

overdoped samples. In the optimally doped sample $x=0.15$ the isotope effect still exists at low temperatures, but it is very small and completely disappears in the overdoped sample $x=0.20$.

To see what happens in samples without Sr doping, we performed the EPR in parent compound $La_2CuO_4$ with different oxygen isotopes. No isotope effect was found for these samples. This result indicates that the holes doped to $CuO_2$ planes are crucial to observe the isotope effect on the EPR signal.

## IV. ORIGIN OF THE EPR LINEWIDTH

The main spin interaction of the Mn ion with other degrees of freedom is an isotropic exchange interaction with neighboring Cu ions:

$$H_{s\sigma}=\frac{1}{2}\sum_{\langle pj\rangle} J_{s\sigma}(\mathbf{S}_p\boldsymbol{\sigma}_j). \tag{1}$$

Here $J_{s\sigma}$ is the exchange integral between Mn and the neighboring Cu ions, $\mathbf{S}_p$ and $\sigma_j/2$ are the spin operators of the Mn and Cu, respectively ($\sigma$ is the Pauli matrix), $\langle pj\rangle$ means the sum over neighboring sites. It is tempting to think that the mechanism of spin relaxation of the Mn ion is similar to the relaxation of nuclear spins coupled by the isotropic hyperfine interaction to the Cu spin-system. However, this naive approach is not valid here. The main difference is that the Larmor frequencies of Mn and Cu ions are very close to each other and the isotropic exchange between them is very strong, being of the same order of magnitude as the isotropic exchange between the Cu ions. In this situation a collective motion of the transverse homogeneous magnetizations of the Mn and Cu ions appears, if the relaxation rate between them $\Gamma_{s\sigma}$ is faster than the relaxation of each of them to the lattice $\Gamma_{sL}$ and $\Gamma_{\sigma L}$: $\Gamma_{s\sigma}\gg\Gamma_{sL},\Gamma_{\sigma L}$ (bottleneck effect). An expression for the relaxation rate $\Gamma_{s\sigma}$ is similar to the well known nuclear relaxation rate $1/T_1$ in which the hyperfine coupling constant $A$ is replaced by $J_{s\sigma}$:[4]

$$\Gamma_{s\sigma}=\left(\frac{J_{s\sigma}}{\hbar}\right)^2\frac{k_BT}{\hbar N}\sum_{\mathbf{q}} F_{\mathbf{q}}^2\,\mathrm{Im}\left[\frac{\chi_\sigma^{\parallel}(\mathbf{q},\omega-\omega_s)}{\omega-\omega_s}+\frac{\chi_\sigma^{\perp}(\mathbf{q},\omega)}{\omega}\right], \tag{2}$$

$$F_{\mathbf{q}}=2(\cos q_x a+\cos q_y a).$$

Here $\chi_\sigma^{\parallel}(\mathbf{q},\omega)$ and $\chi_\sigma^{\perp}(\mathbf{q},\omega)$ are the longitudinal and transverse dynamical spin susceptibilities of the Cu spin system, $N$ is the number of Cu ions in the $CuO_2$ plane, $\mathbf{q}$ is the two-dimensional wave vector, $\omega_s$ is the resonance frequency, and $F_{\mathbf{q}}$ is the form factor. The ratio of electron and nuclear relaxation rates is equal to $(J_{s\sigma}/A)^2$. Therefore one can make a rough estimate of $\Gamma_{s\sigma}$, using an experimental value of the $^{63}Cu$ nuclear relaxation rate $1/T_1$. Taking $J_{s\sigma}=500$ K, $A=100$ kOe/$\mu_B$ and $1/T_1=2700\ \mathrm{s}^{-1}$ (which is doping and temperature independent at high temperatures[6]), we obtain $\Gamma_{s\sigma}\approx 10^{13}\ \mathrm{s}^{-1}$. One can expect that this enormous value provides the condition of the bottleneck regime. At low temperatures $1/T_1\to 0$ for doped samples.[6] The same can be expected for $\Gamma_{s\sigma}$. Consequently at low enough temperatures a partial opening of the bottleneck will take place. In the bottleneck regime the effective relaxation rate $\Gamma_{eff}$ is controlled mainly by the individual relaxation rates of Mn and Cu ions to the lattice $\Gamma_{sL}$ and $\Gamma_{\sigma L}$ weighted by the corresponding static spin susceptibilities:

$$\Gamma_{eff}=\frac{\chi_s^0\Gamma_{sL}+\chi_\sigma^0\Gamma_{\sigma L}}{\chi_s+\chi_\sigma}+\frac{\langle(\Delta\omega)^2\rangle}{\Gamma_{s\sigma}}. \tag{3}$$

The last term takes into account a partial opening of the bottleneck at low temperatures where $\Gamma_{s\sigma}\to 0$. $\langle(\Delta\omega)^2\rangle$ is the mean square of the local fields distribution at the Mn sites. $\chi_s^0$, $\chi_\sigma^0$ and $\chi_s$, $\chi_\sigma$ are the bare and renormalized spin susceptibilities of the Mn and Cu spin systems, respectively. The latter are

$$\chi_{s,\sigma}=\chi_{s,\sigma}^0\frac{1+\lambda\chi_{s,\sigma}^0}{1-\lambda^2\chi_s^0\chi_\sigma^0},\quad \chi_s^0=yN\frac{(g_s\mu_B)^2}{3k_BT},$$
$$\lambda=\frac{2zJ_{s\sigma}}{Ng_sg_\sigma\mu_B^2}, \tag{4}$$

where $g_s$ and $g_\sigma$ are the $g$ factors, $y$ is the concentration of Mn ions, $z$ is the number of their neighboring Cu ions. Usually, $\Gamma_{sL}$ is much smaller than $\Gamma_{\sigma L}$, since the ground state of the $Mn^{2+}$ ion is an orbital $S$ state and the spin-orbit interaction of Mn is rather small. This conclusion was indirectly confirmed experimentally by Kochelaev *et al.*,[4] where the EPR linewidth at high temperatures in such a system was found to be inversely proportional to the concentration of Mn ions [roughly $\chi_s+\chi_\sigma\sim y$ if $\chi_s^0\gg\chi_\sigma^0$ in Eq. (3)]. This finding also provides a direct proof of the bottleneck regime. So, one can conclude that the broadening of the EPR line at high temperatures can mainly be attributed to the relaxation of the Cu transverse magnetization to the lattice $\Gamma_{\sigma L}$. At the same time, the contribution of this relaxation to the EPR linewidth is sufficiently reduced in the bottleneck regime by the factor $\chi_\sigma^0/(\chi_s+\chi_\sigma)<1$. As a matter of fact, the bottleneck effect is used here as a tool to measure the EPR signal of the Cu ions in $La_{2-x}Sr_xCuO_4$ and to understand the mechanism of their spin-lattice relaxation. This is only possible because the Mn ions serve as a local spin probe of the copper spin system.

The nature of the EPR silence of superconducting cuprates and their parent compounds was a subject of intensive theoretical and experimental investigations.[7] In particular, Chakravarty and Orbach[8] and Lazuta[9] proposed that the EPR line in $La_2CuO_4$ is severely broadened below room temperature due to the anisotropic Dzyaloshinskii-Moriya (DM) interactions, but they have concluded that EPR could be observed at elevated temperatures. Simon *et al.*[10] extended the search of the EPR signal in $La_2CuO_{4+\delta}$ up to 1150 K, but no EPR signal was observed. They appeal to an additional contribution to the linewidth broadening at high temperatures because of the modulation of DM interactions due to the change of the Cu-Cu distances by lattice vibrations.[11] However, this contribution is much smaller compared to the static one considered by Chakravarty and Orbach and therefore cannot be the reason for the EPR silence. It seems at this point that any of the models proposed, including a rather exotic ''anyon mechanism'' suggested by Mehran,[12] is not able to explain a very large broadening of the $Cu^{2+}$ EPR signal in the superconducting cuprates and their parent compounds. Furthermore, they cannot explain the huge isotope effect on the linewidth presented in this work.

The isotope effect indicates an important role of the lattice motion in the relaxation of the Cu magnetization. We propose that an interaction between the $Cu^{2+}$ spin system and the lattice motion in general is the same as in insulators, i.e., due to the modulation of the crystal electric field by the lattice distortions and the spin-orbit coupling of the Cu ions. This mechanism usually leads to a rather slow spin-lattice relaxation rate, since the Kramers doublet is not sensitive to the electric field because of time-reversal symmetry. Nonvanishing matrix elements of the spin-lattice coupling appear only due to the external magnetic field. This gives an additional very small factor $g\beta H/\Delta$, where $\Delta$ is the crystal-field splitting of the orbital states. In our case the eigen states of the Cu spin system are defined mainly by the very large isotropic Cu-Cu exchange, instead of the Zeeman interaction. Roughly speaking, the Cu-Cu exchange coupling $J=1500$ K will play the role of the magnetic field splitting $g\beta H$.

The spin-orbit interaction couples the ground state of the $Cu^{2+}$ ion $d(x^2-y^2)$ to the excited states $d(xz)$ and $d(yz)$ only and the relations between the matrix elements are dictated for the Kramers doublet by the time-reversal symmetry. Taking this into account it was found that the Hamiltonian of the spin-lattice interaction has the following form:[1]

$$H_{\sigma L}=\frac{J\Lambda}{8a}\sum_{\langle ij\rangle}[(\sigma_y^i\sigma_z^j-\sigma_z^i\sigma_y^j)(Q_4^i-Q_4^j)+(\sigma_x^i\sigma_z^j-\sigma_z^i\sigma_x^j)(Q_5^i-Q_5^j)], \quad (5)$$

$$\Lambda=\frac{3\lambda G}{\Delta^2}.$$

Here $Q_4^i$ and $Q_5^i$ are the normal coordinates of the oxygen octahedron $CuO_6$, which describe its distortions due to the tunneling motion of the apical oxygen between the four potential minima without the rigid rotation of the octahedra as a whole. The constants $\lambda$ and $G$ correspond to the spin-orbit and orbit-lattice coupling, $\Delta$ is the crystal-field splitting between the ground and excited orbital energy levels, $\langle ij\rangle$ means the sum over neighboring Cu sites in the $x-y$ plane, $a$ is the lattice constant. One can see that $H_{\sigma L}$ has antisymmetric properties of the DM interactions. A similar expression can be obtained in the case of pure rotations of an oxygen octahedron without distortion with $R_x,R_y,R_z$, which correspond to the rotation of octahedron around the $x,y,z$ axes. However, in this case the constant $\Lambda_r$ is much smaller than $\Lambda$.[13] Therefore we omit the contribution of the pure rotations on the spin relaxation to make our consideration less cumbersome.

We calculated the transverse relaxation rate $\Gamma_{\sigma L}$, using the usual decoupling scheme for the correlation functions, taking into account the antisymmetric properties of $H_{\sigma L}$ and antiferromagnetic correlations of the Cu spins,

$$\Gamma_{\sigma L}=\frac{(zJ\Lambda)^2}{64\hbar^2\chi_\sigma^0 k_B T}\int_{-\infty}^{+\infty}d(t-t')\times[\langle Q_4(t)Q_4(t')\rangle+\langle Q_5(t)Q_5(t')\rangle]\times\frac{1}{N}\sum_{\mathbf{q}}\langle\sigma_{st}^{\mathbf{q}}(t)\sigma_{st}^{-\mathbf{q}}(t')\rangle\langle\sigma_{tot}^{-\mathbf{q}}(t)\sigma_{tot}^{\mathbf{q}}(t')\rangle. \quad (6)$$

Here $\sigma_{st}^{\mathbf{q}}/2$ and $\sigma_{tot}^{\mathbf{q}}/2$ are the space Fourier transforms of the staggered and total transverse spin polarizations of the Cu spin system, respectively, $\langle\cdots\rangle$ means an averaging with an equilibrium statistical operator.

In order to find the correlation functions of the involved normal modes $Q_4$ and $Q_5$ we take into account the following considerations. It is well established that $La_{2-x}Sr_xCuO_4$ experiences a structural phase transition from a high-temperature tetragonal (HTT) to a low-temperature orthorhombic (LTO) phase due to the rotations of the neighboring octahedra around the $x-y$ diagonal axis in opposite directions, and further to the low temperature tetragonal (LTT) phase. These structural phase transitions are due to pure rotations $(R_x,R_y,R_z)$ because of an anharmonicity and a very strong coupling of rotations of the neighboring octahedra, which share common oxygen ions in the $CuO_2$ plane. The structural phase transition temperature $T_s$ depends on the tunneling of the rotation motions. The transition occurs if the coupling between rotations of neighboring octahedra dominates over tunneling of rotations for a given octahedron. It was found that even below the HTT-LTO transition temperature, there is a distribution of local tilts of a relatively large magnitude (see Ref. 14 for a review). Having these observations in mind, we propose that the normal modes $Q_4$ and $Q_5$, which describe the tilts of the octahedron $z$ axis, are strongly anharmonic, but the coupling between the neighboring octahedra is weaker compared to pure rotations. Nevertheless, $Q_4/Q_5$ modes are influenced by the structural phase transition, what can be described in terms of the ''molecular field'' $w$, which appears below $T_s$.

Similar to the original work of Thomas and Müller[15] on phase transitions in perovskites, we can write a potential energy $V(Q_4,Q_5)$ in the following form:

$$V(\rho,\theta)=-\frac{1}{2}k\rho^2+\frac{1}{4}\rho^4[u+v(1-\cos 4\phi)]; \qquad (7)$$

$$Q_4=\rho\sin\phi, \quad Q_5=\rho\cos\phi.$$

Here the constants $k>0$ and $u>0$. In the case $v>0$ this potential has four minima at $\rho_0=\sqrt{k/u}$ and $\phi_n=\pi n/2$ with $n=0,1,2,3$. If $v<0$, the minima positions will be the same after the linear transformation to a new coordinate $\phi'=\phi-\pi/4$. It is clear that, besides the radial and azimuthal vibrations near the four minima, there is quantum tunneling between the minima. The azimuthal tunneling frequency $t_0/\hbar$ between the nearest minima is estimated to be

$$t_0=\hbar\Omega\exp(-\zeta); \quad \zeta=\gamma\frac{\rho_0}{\hbar}\sqrt{MV_a}. \qquad (8)$$

Here $\Omega$ is the frequency of vibrations at the bottom of the minima, $\gamma$ is a numerical constant of the order of unity, $M$ is an oxygen mass, $V_a=(1/2)|v|\rho_0^4$ is the azimuthal energy barrier between the minima. The lowest fourfold vibrational level becomes split due to the tunneling into three levels: one twofold level remains unshifted, and two others are shifted at $\pm 2t_0$. The radial tunneling between the minima is less important. At this point static distortions of the octahedra are absent. Below the temperature of a structural phase transition every octahedron experiences a ''molecular field'' due to an elastic interaction between distortions and rotations of the octahedra, which makes the minima nonequivalent. For a particular choice of the molecular field $w$, coupled to the normal coordinate $Q_5=\rho_0\cos\phi$, the only nonzero values for the minima are at $\phi_0=0$ and $\phi_2=\pi$ (after projection on the four lowest eigenstates). Then the correlation functions and static distortions for the normal modes can be expressed in form

$$\langle Q_4|Q_4\rangle_\omega=\langle Q_5|Q_5\rangle_\omega$$
$$=\pi\hbar\rho_0^2\frac{\tanh(t_0/k_BT)}{\exp(\hbar\omega/k_BT)-1}$$
$$\times[\delta(\hbar\omega-2t_0)-\delta(\hbar\omega+2t_0)]; \qquad (9)$$

$$\langle Q_5\rangle=\rho_0\frac{w}{2t_0}\tanh\left(\frac{t_0}{k_BT}\right). \qquad (10)$$

To calculate $\Gamma_{\sigma L}$ defined in Eq. (6) we need now the spin-correlation functions. Unfortunately, the corresponding reliable theory was developed up to now only for the undoped cuprates in terms of a two-dimensional $S=1/2$ quantum Heisenberg antiferromagnet on a square lattice.[16] At the same time, a variety of experimental results on the nuclear-spin relaxation in doped cuprates were successfully described on the basis of the phenomenological expression for the spin susceptibility of Millis, Monien, and Pines (MMP).[17] Using Eqs. (6) and (9) and the MMP model for the spin-correlation functions (see details in Appendix A), we arrive to the following result for the relaxation rate of the total transverse spin of the Cu ions due to the tunneling motion:

$$\Gamma_{\sigma L}^{tun}=\frac{(zJ\Lambda\rho_0)^2\alpha t_0\xi}{2\pi(\hbar a)^2c_1}\left[\sinh\left(\frac{2t_0}{k_BT}\right)\right]^{-1}. \qquad (11)$$

Here $\xi$ is the spin correlation length, $c_1$ is the constant of the order of the spin-wave velocity, and $\alpha$ is the density of states. It is remarkable that at high temperatures, $k_BT\gg 2t_0$, this rate does not depend on the value of the tunneling frequency.

The static DM interaction also gives a contribution to $\Gamma_{\sigma L}$. In fact, it was already considered in Refs. 8 and 9 as the main source of the EPR broadening in the undoped cuprates. This contribution becomes important in comparison with Eq. (11) only at low temperatures, where the latter decreases exponentially. However, at low temperatures the main broadening comes from the second term in Eq. (3) and we omit the contribution of the static DM interactions to $\Gamma_{\sigma L}$.

Our next step will be the calculation of the second term in $\Gamma_{eff}$ given in Eq. (3). We have mentioned already that at high temperatures the effective EPR linewidth decreases with increasing Mn concentration. However, at low temperatures this behavior changes to the opposite: the EPR linewidth becomes proportional to the Mn concentration.[4] At least two conclusions can be made from this observation: (i) the opening of the bottleneck takes place, (ii) the mean square of the local-field distribution $\langle(\Delta\omega)^2\rangle$ is likely to be due to the interaction between the Mn ions. The usual direct magnetic dipole-dipole interactions are too weak to be the reason of the measured line broadening. The indirect interactions via the Cu spin excitations by means the isotropic Mn-Cu exchange coupling in Eq. (1), proposed in Ref. 4 seems to be ruled out too, because of the fast local rotational averaging of the Cu spin susceptibility above the Néel temperature (if there is no local spin texture of the skyrmion type). As a result, the Mn-Mn spin interactions become isotropic and give no contribution to the broadening of the EPR line. A reasonable candidate for the anisotropic spin interaction between the Mn and Cu ions can be the two-particle interaction of the type in Eq. (5). Since the spin-orbit coupling of the Mn ion is rather weak, the $Q_4/Q_5$ distortions of the octahedron around the Cu are important only:

$$H_{s\sigma}^d=\frac{J_{s\sigma}\Lambda}{2a}\sum_{\langle pj\rangle}[(S_y^p\sigma_z^j-S_z^p\sigma_y^j)Q_4^j+(S_x^p\sigma_z^j-S_z^p\sigma_x^j)Q_5^j]. \qquad (12)$$

The result for the second term in Eq. (3) due to the Mn-Mn anisotropic spin interactions via spin fluctuations of the Cu spin system is the following (see details in Appendix B):

$$\frac{\langle(\Delta\omega)^2\rangle}{\Gamma_{s\sigma}}=\frac{yS(S+1)(zJ_{s\sigma})^2\alpha c_1\xi}{12a^2k_BT}\left[\frac{\Lambda\rho_0 w}{2at_0}\tanh\left(\frac{t_0}{k_BT}\right)\right]^4. \qquad (13)$$

This formula is valid if $t_0 \geqslant w$. In the case $t_0 < w$ the situation changes significantly, since every octahedron now is localized in one of the minima, with its population controlled by the temperature. This picture is similar to the transformation of the dynamic Jahn-Teller effect into a static one by the additional splitting of vibronic energy levels by the lattice distortions.[18] So, Eq. (13) has to be modified in this case by the following substitutions:

$$2t_0 \rightarrow \varepsilon = \sqrt{4t_0^2 + w^2}, \quad \tanh^4\left(\frac{t_0}{k_B T}\right) \rightarrow \frac{1}{2}\left[1 + \tanh^2\left(\frac{\varepsilon}{2k_B T}\right)\right]. \tag{14}$$

At low temperatures the second substitution makes no difference, however, it is important for $k_B T \gg \varepsilon$. The same effect of the static picture appears if $t_0 < \Gamma_{s\sigma}$.

## V. COMPARISON OF THE MODEL WITH THE EXPERIMENTAL RESULTS

First of all we estimate the value of the relaxation rate $\Gamma_{\sigma L}$ given in Eq. (11) at high temperatures in order to find out whether the proposed mechanism due to the azimuthal tunneling motion of the octahedra is effective enough to give a large broadening of the EPR line. We expect that at $T = 200$ K the rate $\Gamma_{\sigma L}$ does not depend on $t_0$ because of the relation $t_0 \ll k_B T$. For our estimation we take the orbit-lattice coupling $G \approx 2\Delta$, where $\Delta$ is the crystal-field splitting between the ground and excited orbital energy levels.[19] The spin-orbit coupling and the exchange Cu-Cu integral are well known:[19] $\lambda/\Delta \approx 0.066$ and $J = 1500$ K. A value of the radial position of the minima $\rho_0$ (the projection of the apical oxygen onto the $x-y$ plane), which is expected to be of the same order of magnitude as for the octahedra rotations at the structural phase transition, we take $\rho_0 = 0.1 \times 10^{-8}$ cm. The parameters of the MMP model were estimated in Ref. 17 from NMR experiments. For a doping level $x = 0.1$ we have $\alpha\xi/c_1 = 2.26 \times 10^3/\mathrm{eV}^2$. Inserting all these values into Eq. (11), we obtain $\Gamma_{\sigma L} \approx 1.7 \times 10^{11}\ \mathrm{s}^{-1}$, or the expected EPR linewidth in $La_{2-x}Sr_xCuO_4$ (without Mn) is $\Delta H_{\sigma L} = \hbar\Gamma_{\sigma L}/2\mu_B \approx 0.9 \times 10^4$ Oe. For $x = 0.15$, $\alpha\xi/c_1 = 2 \times 10^3/\mathrm{eV}^2$ and $\Delta H_{\sigma L} \approx 0.8 \times 10^4$ Oe. These values are too large for observing an EPR signal at the usual frequencies. In addition, the EPR intensity is proportional to the susceptibility $\chi_\sigma^0$, which is very small in cuprates. This can explain the EPR silence of $La_{2-x}Sr_xCuO_4$ and similar compounds.

It was explained above that the samples doped with Mn show an EPR signal with a linewidth reduced by the factor $\chi_\sigma^0/(\chi_s + \chi_\sigma)$ at high temperatures due to the bottleneck effect. Interesting high-precision susceptibility measurements of $\chi_\sigma^0$ for $La_{2-x}Sr_xCuO_4$ were performed by Müller *et al.*[21] with $x$ in the range $0.06 \leqslant x \leqslant 0.2$. The experimental values for $\chi_s + \chi_\sigma$ are available for the Mn concentrations $0.01 \leqslant y \leqslant 0.06$ and $0 \leqslant x \leqslant 0.30$, being not very sensitive to the Sr content.[4] In our case with $y = 0.02$, $\chi_s + \chi_\sigma = 5.7 \times 10^{-7}$ emu/g at $T = 200$ K. If we take $\chi_\sigma^0 = 1.3 \times 10^{-7}$ emu/g for $x = 0.09$, we obtain $\Delta H_{eff} = \chi_\sigma^0/(\chi_s + \chi_\sigma)\Delta H_{\sigma L} \approx 2 \times 10^3$ Oe. This value can be compared with our experimental result $\Delta H_{pp} = 1.2 \times 10^3$ Oe for the $x = 0.10$ sample. For optimal doping, $x = 0.15$, we have $\chi_\sigma^0 = 2.3 \times 10^{-7}$ emu/g and $\Delta H_{eff} = 3.1 \times 10^3$ Oe, which can be compared with our result of $\Delta H_{pp} = 1.35 \times 10^3$ Oe. We find that the agreement is reasonable, having in mind an uncertainty of the constants used. These estimations show that the proposed mechanism of the $Cu^{2+}$ EPR broadening is effective enough at high temperatures, what was a long-standing problem up to now.

At low temperatures the tunneling motion is less effective and the second term in $\Gamma_{eff}$ due to the partial opening of the bottleneck in Eq. (13) plays the main role. We estimate it for the sample with $x = 0.1$ at $T = 10$ K. Besides the constants used above, we take $y = 0.02$, $J_{s\sigma} \approx 500$ K, and $S = 5/2$. It seems, however, that we should take a larger value for $\rho_0$ at low temperatures. Recently, Bianconi *et al.*[3] have found that below a characteristic temperature $T^* = 100$ K about one-third of all octahedra in the sample with $x = 0.15$ have a tilting angle $\theta = 16°$ instead of $\theta = 5°$ after the HTT→LTO transition. A similar observation was made by Lanzara *et al.*[22] from x-ray-absorption near-edge structure (XANES) in the sample with $x = 0.06$, where $T^*$ increases from 110 to 170 K upon replacing $^{16}O$ with $^{18}O$. One can expect that a similar effect will happen with $Q_4/Q_5$ distortions and we take $\rho_0 = 0.3$ Å. We use also the MMP parameters $\alpha c_1 \xi/a^2 \approx 100$ and $w = 2t_0$. Inserting all these values in Eq. (13) gives $\Delta H \approx 1.1 \times 10^3$ Oe. This value has to be compared with our experimental result $\Delta H = 2 \times 10^3$ Oe at $T = 10$ K for $x = 0.1$. The agreement is reasonable, since we have omitted the pure rotations, which can give a noticeable contribution at low temperatures. The above considerations show that our model is able to give a reasonable agreement with the observed EPR linewidth at high and low temperatures.

## VI. TEMPERATURE AND DOPING DEPENDENCE OF THE EPR LINEWIDTH

To describe the temperature dependence of the EPR linewidth with our theoretical model, it is necessary to make a definite conclusion on the temperature dependence of the spin-correlation length $\xi(T)$. Barzykin and Pines[20] have found from the NMR measurements that in underdoped samples $\xi(T)$ is given by

$$\frac{\xi_0}{\xi(T)} = 1 + \frac{T}{T_\xi}, \tag{15}$$

where $\xi_0$ and $T_\xi$ are constants, both depending on the doping level. This behavior agrees qualitatively with the quantum Heisenberg antiferromagnet theory for the quantum critical regime.[16] It is important to point out that although such a behavior is acceptable for the underdoped samples, it breaks down for the doping level $x < 0.02$, where the spin-correlation length becomes exponentially divergent. This will change the spin dynamics of our system, since it remains now in the deep bottleneck regime even at very low temperatures.

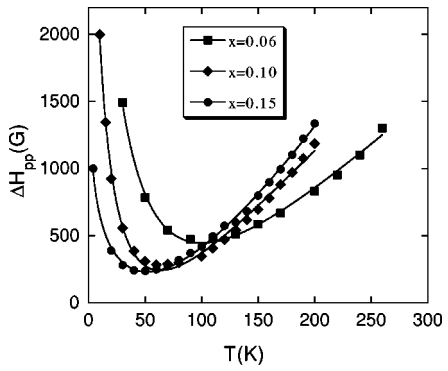


FIG. 5. Temperature dependence of the EPR linewidth $\Delta H_{pp}$ for $^{16}O$ isotope samples of $La_{2-x}Sr_xCu_{0.98}Mn_{0.02}O_4$ with $x=0.06$, 0.10, and 0.15. The solid lines represent the best fit to Eq. (17) with parameters listed in Table I.

The spin susceptibilities involved in $\Gamma_{eff}$ also depend on temperature. According to Ref. 21, $\chi_\sigma^0$ in our temperature range can be approximated by a linear function and $1/(\chi_s+\chi_\sigma)$ was found to be proportional to temperature.[4] So, we can take

$$\frac{\chi_\sigma^0}{\chi_s+\chi_\sigma}=CT\left(1+\frac{T}{T_\chi}\right), \tag{16}$$

where $C$ and $T_\chi$ are doping dependent constants. Using Eqs. (3), (11), and (13) we can write the fitting function for the static regime according to Eq. (14)

$$\Delta H_{eff}=\left\{A\frac{{t_0}^2 T}{\varepsilon\sinh(\varepsilon/T)}\left(1+\frac{T}{T_\chi}\right)+\frac{B}{T}\left(\frac{w}{\varepsilon}\right)^4\left[1+\tanh^2\left(\frac{\varepsilon}{2T}\right)\right]\right\}\left(1+\frac{T}{T_\xi}\right)^{-1}; \tag{17}$$

$$\varepsilon=\sqrt{4{t_0}^2+w^2}.$$

Here $A$, $B$, $t_0$, and $w$ are fitting parameters. Figure 5 shows the linewidth data and the corresponding fitted curves using Eq. (17) for the samples with $x=0.06$, 0.10, 0.15. One can see that the agreement is good. To reduce the number of fitting parameters we took $T_\xi=34$ K according to Ref. 20 and the molecular field $w=10$ K for all doping levels. The fitting parameters together with the values $T_\chi$ from Ref. 21 are listed in Table I.

TABLE I. The fitting parameters of the EPR linewidth $\Delta H_{pp}$ in $La_{2-x}Sr_xCu_{0.98}Mn_{0.02}O_4$ using Eq. (17). The molecular field parameter $w$ and the parameter $T_\xi$ defined in Eq. (15) are taken to be $w=10$ K and $T_\xi=34$ K (see text).

| Sr doping | $T_\chi$(K) [a] | $A\times10^3$(kOe/K$^2$) | $B\times10^{-3}$(kOe K) |
|---|---|---|---|
| $x=0.06$ | 560 | 0.432 | 100.8 |
| $x=0.1$ | 320 | 0.504 | 182.2 |
| $x=0.15$ | 484 | 0.663 | 95.57 |

[a] $T_\chi$ is extracted from Ref. 21; see Eq. (16).

## VII. THE ISOTOPE EFFECT

The isotope effect appears in our model due to the exponential dependence of the tunneling frequency $t_0=\hbar\Omega\exp(-\zeta)$ given in Eq. (8) on $\zeta$ and thus on the oxygen mass $M$. Also frequency of the vibrations near the potential minima $\Omega$ depends on $M$, $\Omega\sim1/\sqrt{M}$. For $x=0.06$ sample we observed an isotope effect on EPR linewidth $(^{18}\Delta H)/(^{16}\Delta H)=1.2$ at $T=50$ K. Using this experimental value and taking $\rho_0=0.1$ Å, we obtain from Eq. (13) the reasonable value of the potential barrier between the minima $V_a=300$ K.

According to Eq. (11), the isotope effect is absent at high temperatures, in agreement with the experimental results. Using our model it is also possible to understand the doping dependence of the isotope effect. It is well known that the hole doping strongly reduces the temperature of the structural phase transition. Therefore one can expect that the value of the potential barrier $V_a$ decreases with doping. The latter reduces the value of $\zeta$. This results in a fast increase of the tunneling frequency $t_0$, as well as in a reduction of the isotope effect. Moreover, the increase of $t_0$ leads to a decrease of the second term in $\Gamma_{eff}$ in Eq. (3), shifting the minimum in the EPR linewidth towards low temperatures. In the undoped sample the isotope effect disappears because of two reasons: First, the potential barrier becomes so high that $t_0\ll w$. Second, what is more important, the Cu spin-system enters in the renormalized classical regime with the exponential divergence of the spin-correlation length $\xi$ at low temperatures. In this case the main contribution to the EPR linewidth at low temperatures arises from the first term in Eq. (3), since $\Gamma_{\sigma L}$ is now proportional to $\xi^3$ due to the usual magnetic dipole-dipole interaction.[8,9] All these predictions of this model are clearly observed in the present experiments.

From the above it is clear that the relaxation of the $Cu^{2+}$ spins via the $Q_4/Q_5$ tilting modes due to the interaction given in Eq. (5) can explain the isotope effect on the EPR linewidth. In a recent EPR study on $La_{2-x}Sr_xCuO_4$ broad lines were observed, which were analyzed in terms of a $S=1/2$ three-spin polaron, consisting of two $Cu^{2+}$ ions and one oxygen hole.[2] The essential part of the analysis is a dynamical $Q_2$ mode distortion of the oxygen square around a $Cu^{2+}$ ion in the $CuO_2$ plane. Therefore the question arises what is the relation of the $Q_4/Q_5$ dynamics with the $Q_2$ one. At this point the local structural information gained by EXAFS is of relevance.[3] The time scale of this x-ray technique is $10^{-15}$ s, i.e., quasi-instantaneous. With this technique two local octahedral deformations were detected: (i) a quasi-tetragonal distortion (distortion A), assigned to metallic stripes with high hole concentration, and (ii) an octahedral distortion (distortion B), in which the Cu-O squares are $Q_2$ distorted. Due to the elongation along one direction the $CuO_4$ platelet of the $CuO_6$ octahedra gets tilted out of the plane by $Q_4/Q_5$ rotation (see Fig. 6). Therefore there is a *sterically induced linear relationship between the planar Jahn-Teller $Q_2$ distortion and the $Q_4/Q_5$ tilting of the octahedra*, causing the $Cu^{2+}$ EPR relaxation. Site selective oxygen isotope studies showed that up to 80% of the isotope shift on $T_c$ is due to the planar oxygens.[23] Thus it is clear that

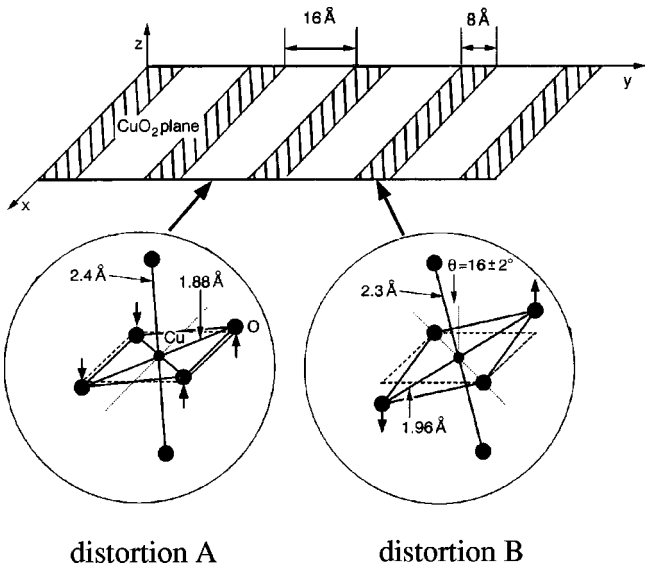


FIG. 6. Schematic view of the distorted $CuO_6$ octahedra based on EXAFS measurements (Ref. 3). Left side: octahedra with a quasitetragonal distortion (distortion A). Right side: octahedra with an octahedral distortion (distortion B). Note that the planar $Q_2$ distortion sterically induces large tilting $Q_4/Q_5$ mode.

the pairing mechanism occurs in the $CuO_2$ plane. However, the EPR relaxation through the $Q_4/Q_5$ tilting is related to this pairing interaction.

## VIII. SUMMARY

In summary, we studied the EPR in $Mn^{2+}$ doped $La_{2-x}Sr_xCuO_4$ with $^{16}O$ and $^{18}O$ oxygen isotopes. We observed that the EPR linewidth is isotope dependent. The linewidth for the $^{18}O$ sample is larger than for the $^{16}O$ sample. The isotope effect is large in underdoped region. With increasing Sr doping the isotope effect decreases and disappears in the overdoped regime.

In order to explain the observed isotope effects, a theoretical model is proposed which relates the EPR linewidth with the tilting and tunneling modes of the oxygen octahedra around the copper. This model leads to a Hamiltonian in which the $Q_4$ and $Q_5$ modes are coupled linearly to Dzyaloshinsky-type spin terms. This new theoretical approach allows an estimation of the intrinsic antiferromagnetically coupled EPR relaxation time, and provides an explanation for the long-standing problem of EPR silence in high-$T_c$ cuprates. Furthermore, the observed large isotope effect on the EPR linewidth can be quantitatively accounted for by this theory.

The relaxing $Q_4/Q_5$ local rotational modes are coupled sterically and linearly to the in-plane $Q_2$ quadrupolar modes. These $Q_2$ modes are Jahn-Teller active and considered as relevant for the (bi)polaron formation in the cuprates and therefore for the occurrence of the high-temperature superconductivity.[24]

## ACKNOWLEDGMENTS

We would like to thank O. Schirmer for carefully reading the manuscript which has led to clarifications in the text. We also thank Guo-meng Zhao for valuable discussions. One of the authors (B.I.K.) wishes to thank Zürich University for its hospitality. This work was supported by the Swiss National Science Foundation (Grant Nos. 7 IP 51830 and 20-55.615.98).

## APPENDIX A

The improved MMP expression[20] for the staggered spin susceptibility is

$$\chi_\sigma(\mathbf{q},\omega)=\frac{\alpha\xi^2}{1+\mathbf{q}^2\xi^2-(\omega/\Delta)^2-i(\omega/\omega_{\mathrm{SF}})}, \qquad \text{(A1)}$$

where $\xi$ is the spin correlation length, $\alpha$ is the density of states, $\Delta=c/\xi$ is the gap in the spectrum of the spin-wave excitations with a velocity $c$, and $\omega_{\mathrm{SF}}$ is the characteristic frequency of the damping of the spin excitations $\omega_{\mathrm{SF}}=c_1/\xi$ with the constant $c_1$ of the order $c$. The time Fourier transform of the staggered spin-correlation function is defined by the spin susceptibility by the general relation

$$\frac{1}{4}\langle\sigma_{st}^{\mathbf{q}}\sigma_{st}^{-\mathbf{q}}\rangle_\omega=\frac{2\hbar}{\exp(\hbar\omega/k_{\mathrm{B}}T)-1}\,\mathrm{Im}\,\chi_\sigma(\mathbf{q},\omega). \qquad \text{(A2)}$$

In a similar way we have for the spin-correlation function for the total spin

$$\frac{1}{4}\langle\sigma_{tot}^{\mathbf{q}}\sigma_{tot}^{-\mathbf{q}}\rangle_\omega=\frac{2\hbar\chi_\sigma^0}{\exp(\hbar\omega/k_{\mathrm{B}}T)-1}\,\mathrm{Im}\,\frac{\Gamma_{\mathbf{q}}}{\Gamma_{\mathbf{q}}-i\omega}, \qquad \text{(A3)}$$

where the damping $\Gamma_{\mathbf{q}}$ in the hydrodynamical approximation is $\Gamma_{\mathbf{q}}=Dq^2$. As a matter of fact, the final expression is not sensitive to this approximation in the calculation of $\Gamma_{\sigma L}$ in Eq. (6), if $\Gamma_{\mathbf{q}}\ll\omega_{\mathrm{SF}}$. Inserting Eqs. (A1)–(A3) and (9) into Eq. (6), we obtain

$$\Gamma_{\sigma L}^{tun}=\frac{(zJ\Lambda\rho_0)^2}{4\pi\hbar a^2}\,\frac{\alpha}{\sinh(2t_0/k_{\mathrm{B}}T)}\times\left[\frac{\pi}{2}-\arctan\left(\frac{\omega_{\mathrm{SF}}}{2t_0}-\frac{2t_0\omega_{\mathrm{SF}}}{\Delta^2}\right)\right]. \qquad \text{(A4)}$$

In the case $2t_0\ll\omega_{\mathrm{SF}}\ll\Delta$ we obtain Eq. (11) given in the text.

## APPENDIX B

The interaction between the Mn ions due to the anisotropic Mn-Cu coupling $H_{s\sigma}^d$ [Eq. (12)] via the spin fluctuations of the Cu spin system can be written in the form

$$H_{ss}^d=\frac{(J_{s\sigma}\Lambda)^2}{4a^2N}\sum_{\mathbf{pr}}\sum_{\mathbf{q}}F_{\mathbf{q}}^2\chi_\sigma(\mathbf{q})e^{i\mathbf{q}(\mathbf{p}-\mathbf{r})}\times[2|\langle Q_+\rangle|^2(\mathbf{S_pS_r}+S_{\mathbf{p}}^zS_{\mathbf{r}}^z)+(\langle Q_+\rangle^2S_{\mathbf{p}}^-S_{\mathbf{r}}^-+\langle Q_-\rangle^2S_{\mathbf{p}}^-S_{\mathbf{r}}^-)]. \qquad \text{(B1)}$$

Here $\chi_\sigma(\mathbf{q})=\chi_\sigma(\mathbf{q},\omega=0)$, $F_{\mathbf{q}}$ is the form factor from Eq. (2), and

$$S^{\pm}=S^{x}\pm iS^{y},\quad Q_{\pm}=Q_{5}\pm iQ_{4}.$$

We have taken into account that the nonzero value of the normal modes of different octahedra equals to their static value, induced by the structural transition.

The mean square of the local-fields distribution $\langle(\Delta\omega)^2\rangle_d$ due to the interaction $H_{ss}^{d}$ is

$$\langle(\Delta\omega)^2\rangle_d=\frac{\langle[S^+,H_{ss}^d][H_{ss}^d,S^-]\rangle_0}{\langle S^+S^-\rangle_0},\quad S^{\pm}=\sum_{\mathbf{p}}(S_{\mathbf{p}}^{x}\pm iS_{\mathbf{p}}^{y}), \tag{B2}$$

where $[A,B]=AB-BA$, $\langle\cdots\rangle_0$ means an averaging with unperturbed statistical operator. The result is the following:

$$\langle(\Delta\omega)^2\rangle=\frac{y}{6}S(S+1)\left(\frac{J_{s\sigma}\Lambda|\langle Q_+\rangle|}{a}\right)^4\left[\frac{1}{N}\sum_{\mathbf{q}}F_{\mathbf{q}}^4\chi_{\mathbf{q}}^2-\left(\frac{1}{N}\sum_{\mathbf{q}}F_{\mathbf{q}}^2\chi_{\mathbf{q}}\right)^2\right]. \tag{B3}$$

Here $y$ is the Mn concentration. This expression is similar to the formula obtained by Thelen and Pines[25] for the transverse nuclear-spin relaxation rate. They have shown that the second term in Eq. (B3) can be neglected. Substituting $\chi_{\mathbf{q}}=\chi_{\sigma}(\mathbf{q})$ from Eq. (A1), we have in the case of HTT→LTO transition

$$\langle(\Delta\omega)^2\rangle=\frac{y}{24\pi}S(S+1)\left(\frac{zJ_{s\sigma}\Lambda\langle Q_5\rangle}{a}\right)^4\left(\frac{\alpha\xi}{\hbar a}\right)^2. \tag{B4}$$

Now we need an explicit expression for the relaxation rate between the Mn and Cu spin systems due to the isotropic exchange interaction $\Gamma_{s\sigma}$. Substituting Eq. (A1) into Eq. (2), we have

$$\Gamma_{s\sigma}=\frac{1}{2\pi}\left(\frac{zJ_{s\sigma}}{\hbar}\right)^2\frac{\alpha k_BT}{\omega_{SF}}. \tag{B5}$$

Finally, substituting $\omega_{SF}$ and $\langle Q_5\rangle$, we obtain

$$\frac{\langle(\Delta\omega)^2\rangle}{\Gamma_{s\sigma}}=\frac{yS(S+1)(zJ_{s\sigma})^2\alpha c_1\xi}{12a^2k_BT}\left[\frac{\Lambda\rho_0 w}{2at_0}\tanh\left(\frac{t_0}{k_BT}\right)\right]^4, \tag{B6}$$

given in the text as Eq. (13).


[1] B. I. Kochelaev, J. Supercond. **12**, 53 (1999).

[2] B. I. Kochelaev, J. Sichelschmidt, B. Elschner, W. Lemor, and A. Loidl, Phys. Rev. Lett. **79**, 4274 (1997).

[3] A. Bianconi, N. L. Saini, A. Lanzara, M. Missori, T. Rossetti, H. Oyanagi, H. Yamaguchi, K. Oka, and T. Ito, Phys. Rev. Lett. **76**, 3412 (1996).

[4] B. I. Kochelaev, L. Kan, B. Elschner, and S. Elschner, Phys. Rev. B **49**, 13 106 (1994).

[5] A. Shengelaya, H. Keller, K. A. Müller, B. I. Kochelaev, and K. Conder (unpublished).

[6] T. Imai, C. P. Slichter, K. Yoshimura, and K. Kosuge, Phys. Rev. Lett. **70**, 1002 (1993).

[7] F. Mehran and P. W. Anderson, Solid State Commun. **71**, 29 (1989).

[8] S. Chakravarty and R. Orbach, Phys. Rev. Lett. **64**, 224 (1991).

[9] A. V. Lazuta, Physica C **181**, 127 (1991).

[10] P. Simon, J. M. Bassat, S. B. Oseroff, Z. Fisk, S.-W. Cheong, A. Wattiaux, and S. Schultz, Phys. Rev. B **48**, 4216 (1993).

[11] T. G. Castner, Jr. and M. S. Seehra, Phys. Rev. B **4**, 38 (1971).

[12] F. Mehran, Phys. Rev. B **46**, 5640 (1992).

[13] This follows from a simple crystal-field consideration: the constant $G$ in Eq. (5) appears in the second order of expansion in terms of $d$-electron coordinates, while the constant of the orbit-rotation coupling $G_r$ appears only in the fourth order. As a result, $G_r/G\simeq\langle r^4\rangle/\langle r^2\rangle R^2\approx 0.2$, where $\langle\cdots\rangle$ means an averaging over $d$-electron wave functions and $R=a/2$ is the distance between the Cu and oxygen ions.

[14] M. K. Crawford, R. L. Harlow, E. M. McCarron, S. W. Tozer, Q. Huang, D. E. Cox, and Q. Zhu, in *High-$T_c$ Superconductivity: Ten Years After the Discovery*, edited by E. Kaldis, E. Liarokapis, and K. A. Müller (Kluwer Academic Publishers, Dordrecht, 1997), p. 281.

[15] H. Thomas and K. A. Müller, Phys. Rev. Lett. **21**, 1256 (1968).

[16] S. Chakravarty, B. Halperin, and D. R. Nelson, Phys. Rev. B **39**, 2344 (1989); P. Hasefratz and F. Niedermayer, Phys. Lett. B **268**, 231 (1991); A. V. Chubukov, S. Sachdev, and J. Ye, Phys. Rev. B **49**, 11 919 (1994); S. I. Belov and B. I. Kochelaev, Solid State Commun. **103**, 249 (1997); **106**, 207 (1998).

[17] A. J. Millis, H. Monien, and D. Pines, Phys. Rev. B **42**, 167 (1990).

[18] F. S. Ham, Phys. Rev. **166**, 307 (1968).

[19] A. Abragam and B. Bleaney, *Electron Paramagnetic Resonance of Transition Ions* (Clarendon Press, Oxford, 1970).

[20] V. Barzykin and D. Pines, Phys. Rev. B **52**, 13 585 (1995).

[21] K. A. Müller, Guo-meng Zhao, K. Conder, and H. Keller, J. Phys.: Condens. Matter **10**, L291 (1998).

[22] A. Lanzara, Guo-meng Zhao, N. L. Saini, A. Bianconi, K. Conder, H. Keller, and K. A. Müller, J. Phys.: Condens. Matter **11**, L541 (1999).

[23] D. Zech, H. Keller, K. Conder, E. Kaldis, E. Liarokapis, N. Poulakis, and K. A. Müller, Nature (London) **371**, 681 (1994).

[24] K. A. Müller, J. Supercond. **12**, 3 (1999).

[25] D. Thelen and D. Pines, Phys. Rev. B **49**, 3528 (1994).